university of groningen

University Medical Center Groningen

University of Groningen

Effect of defect energy on strain-gradient predictions of confined single-crystal plasticity

Nicola, L; Van der Giessen, E; Gurtin, Morton E.

Published in:
Journal of the Mechanics and Physics of Solids

DOI:
10.1016/j.jmps.2005.02.001

IMPORTANT NOTE: You are advised to consult the publisher's version (publisher's PDF) if you wish to cite from it. Please check the document version below.

Document Version
Publisher's PDF, also known as Version of record

Publication date:
2005

Link to publication in University of Groningen/UMCG research database

Citation for published version (APA):
Nicola, L., Van der Giessen, E., & Gurtin, M. E. (2005). Effect of defect energy on strain-gradient predictions of confined single-crystal plasticity. *Journal of the Mechanics and Physics of Solids*, *53*(6), 1280-1294. https://doi.org/10.1016/j.jmps.2005.02.001

Copyright
Other than for strictly personal use, it is not permitted to download or to forward/distribute the text or part of it without the consent of the author(s) and/or copyright holder(s), unless the work is under an open content license (like Creative Commons).

The publication may also be distributed here under the terms of Article 25fa of the Dutch Copyright Act, indicated by the “Taverne” license. More information can be found on the University of Groningen website: https://www.rug.nl/library/open-access/self-archiving-pure/taverne-amendment.

Take-down policy
If you believe that this document breaches copyright please contact us providing details, and we will remove access to the work immediately and investigate your claim.

Downloaded from the University of Groningen/UMCG research database (Pure): http://www.rug.nl/research/portal. For technical reasons the number of authors shown on this cover page is limited to 10 maximum.

Download date: 22-03-2023

Available online at www.sciencedirect.com
SCIENCE DIRECT®
Journal of the Mechanics and Physics of solids
53 (2005) 1280–1294
JOURNAL OF THE MECHANICS AND PHYSICS OF SOLIDS
www.elsevier.com/locate/jmps

Effect of defect energy on strain-gradient predictions of confined single-crystal plasticity

Lucia Nicola[a], Erik Van der Giessen[a,*], Morton E. Gurtin[b]

[a]*The Materials Science Center/The Netherlands Institute for Metals Research, University of Groningen, Nyenborgh 4, 9747 AG Groningen, The Netherlands*
[b]*Department of Mathematical Sciences, Carnegie Mellon University, Pittsburgh, PA 15213, USA*

Received 1 October 2004; received in revised form 31 January 2005; accepted 5 February 2005

Abstract

Gurtin recently proposed a strain-gradient theory for crystal plasticity in which the gradient effect originates from a defect energy that characterizes energy storage due to the presence of a net Burgers vector. Here we consider a number of different possibilities for this energy: specifically, working within a simple two-dimensional framework, we compare predictions of the theory with results of discrete-dislocation simulations of stress relaxation in thin films. Our objective is to investigate which specific defect energies are capable of capturing the size-dependent response of such systems for different crystal orientations.
© 2005 Elsevier Ltd. All rights reserved.

Keywords: Dislocations; Crystal plasticity; Non-local plasticity

1. Introduction

Plastic deformation in confined geometries at the (sub-) micrometer scale is almost always size dependent, albeit for different reasons (see e.g. Hutchinson, 2000; Needleman, 2000). Possible sources are plastic strain gradients associated with the presence of a net Burgers vector in the dislocation distribution, and hence the

*Corresponding author. Tel.: +31 50 363 8047; fax: +31 50 363 4886.
E-mail address: E.van.der.Giessen@rug.nl (E. Van der Giessen).

0022-5096/$ - see front matter © 2005 Elsevier Ltd. All rights reserved.
doi:10.1016/j.jmps.2005.02.001

formation of geometrically necessary dislocations. These features influence plastic flow through lattice curvature and through back stress.

Discrete-dislocation plasticity accounts for these phenomena in a natural manner. Standard continuum plasticity does not, but various strain-gradient plasticity theories have been formulated, including single-crystal theories, e.g. Aifantis (1992), Gurtin (2002), Svendsen (2002), and Gudmundson (2004). The formulations of those theories differ, but some share the property that they explicitly use a free energy that depends on the net Burgers vector, e.g. Gurtin (2002) and Svendsen (2002). This dependence is constitutive, and there are no guidelines other than objectivity, material symmetry and physical insight.

In the present paper, we discuss these issues for the example of the Gurtin (2002) theory and focus on the gradient effect in thin films caused solely by the net Burgers vector of dislocations. Previous results of discrete-dislocation simulations (Nicola et al., 2003, 2005) are considered as numerical data to fit the constitutive moduli appearing in Gurtin's theory. Different expressions for the defect energy in Gurtin's theory are proposed and discussed in the light of their capability to capture the size-dependent response of single-crystalline films at different crystal orientations. The findings are supplementary to a similar comparison by Bittencourt et al. (2003) in aiming to assist in the further development of the theory.

2. Basic equations of Gurtin's theory

The theory (Gurtin, 2002) is meant to characterize single crystals undergoing plastic flow resulting from slip on specified slip systems. Here we restrict attention to the rate-independent material response, neglecting changes in geometry.

The theory is based on the standard crystalline decomposition

$$\nabla \boldsymbol{u} = \boldsymbol{H}^{\mathrm{e}} + \boldsymbol{H}^{\mathrm{p}}, \quad \boldsymbol{H}^{\mathrm{p}} = \sum_{\beta} \gamma^{(\beta)} \mathbb{S}^{(\beta)} \tag{1}$$

of the displacement gradient $\nabla \boldsymbol{u}$ into elastic and plastic parts, $\boldsymbol{H}^{\mathrm{e}}$ and $\boldsymbol{H}^{\mathrm{p}}$, where $\gamma^{(\beta)}$ represents the slip on slip system β. The Schmid tensor $\mathbb{S}^{(\beta)}$ has the form

$$\mathbb{S}^{(\beta)} = \boldsymbol{s}^{(\beta)} \otimes \boldsymbol{m}^{(\beta)}, \quad |\boldsymbol{s}^{(\beta)}| = |\boldsymbol{m}^{(\beta)}| = 1, \quad \boldsymbol{s}^{(\beta)} \perp \boldsymbol{m}^{(\beta)}, \tag{2}$$

where $\boldsymbol{s}^{(\beta)}$ is the slip direction and $\boldsymbol{m}^{(\beta)}$ is the slip-plane normal, both constant in space and time.

The governing equations—derived from a formulation of the principle of virtual work that allows for microstress fields $\pi^{(\beta)}$ and $\boldsymbol{\xi}^{(\beta)}$, respectively, work-conjugate to slips $\gamma^{(\beta)}$ and slip gradients $\nabla \gamma^{(\beta)}$—consist of the classical equilibrium condition

$$\operatorname{div} \boldsymbol{\sigma} = 0, \tag{3}$$

supplemented by the microforce balance

$$\operatorname{div} \boldsymbol{\xi}^{(\beta)} - \pi^{(\beta)} + \tau^{(\beta)} = 0, \quad \tau^{(\beta)} = \mathbb{S}^{(\beta)} \cdot \boldsymbol{\sigma}. \tag{4}$$

The requirement that the increase in free energy not be greater than the rate of work leads to the free-energy inequality

$$\dot{\psi} - \boldsymbol{\sigma} \cdot \dot{\boldsymbol{\varepsilon}}^{\mathrm{e}} - \sum_{\beta} (\boldsymbol{\xi}^{(\beta)} \cdot \boldsymbol{\nabla}\dot{\gamma}^{(\beta)} + \pi^{(\beta)}\dot{\gamma}^{(\beta)}) \leqslant 0, \tag{5}$$

where ψ is the free energy (per unit volume) and $\boldsymbol{\varepsilon}^{\mathrm{e}}$, the elastic strain, is the symmetric part of $\boldsymbol{H}^{\mathrm{e}}$. Here, in contrast to the classical crystalline theory, ψ is taken to have the additive form

$$\psi = \tfrac{1}{2}\boldsymbol{\varepsilon}^{\mathrm{e}} \cdot \mathscr{C}\boldsymbol{\varepsilon}^{\mathrm{e}} + \Psi_{\mathrm{D}} \tag{6}$$

with strain energy augmented by a defect energy Ψ_{D}, which we assume to be quadratic in the slip-gradients $\boldsymbol{\nabla}\gamma^{(\beta)}$. Here $\mathscr{C}$ is the standard fourth-order tensor of elastic moduli, which, assuming elastic isotropy, we express in terms of Young's modulus E and Poisson's ratio ν.

Guided by the classical theory and by the free-energy inequality (5), $\boldsymbol{\sigma}$, $\boldsymbol{\xi}^{(\beta)}$ and $\pi^{(\beta)}$ are presumed given by the constitutive equations

$$\boldsymbol{\sigma} = \mathscr{C}\boldsymbol{\varepsilon}^{\mathrm{e}}, \quad \boldsymbol{\xi}^{(\beta)} = \frac{\partial \Psi_{\mathrm{D}}}{\partial \boldsymbol{\nabla}\gamma^{(\beta)}}, \quad \pi^{(\beta)} = \varphi^{(\beta)} \operatorname{sgn} \dot{\gamma}^{(\beta)}, \tag{7}$$

in which slip-system hardening, as described by the internal variables $\varphi^{(\beta)}$, is here taken to be of the simple (local) form

$$\dot{\varphi}^{(\beta)} = \sum_{\kappa} H_0 |\dot{\gamma}^{(\kappa)}|, \quad \varphi^{(\beta)}|_{t=0} = \pi_0 \tag{8}$$

with π_0 being the initial yield strength.

3. Macroscopic defect measures in plane strain

With a view toward comparison with two-dimensional discrete-dislocation simulations, *we henceforth restrict attention to plane strain*, with deformation occurring in the (x_1, x_2) plane, so that $\boldsymbol{e}_3$ is the out-of-plane direction.

3.1. Burgers vector

The macroscopic Burgers vector is characterized by the Burgers tensor

$$\boldsymbol{G} = \operatorname{curl} \boldsymbol{H}^{\mathrm{p}} = \sum_{\alpha} (\boldsymbol{\nabla}\gamma^{(\alpha)} \times \boldsymbol{m}^{(\alpha)}) \otimes \boldsymbol{s}^{(\alpha)}, \tag{9}$$

which, because here we restrict attention to plane strain, has the simple form

$$\boldsymbol{G} = \boldsymbol{e}_3 \otimes \boldsymbol{g}, \quad \boldsymbol{g} = \sum_{\beta} \partial^{(\beta)}\gamma^{(\beta)}\boldsymbol{s}^{(\beta)}. \tag{10}$$

Here, for each slip system β, $\partial^{(\beta)}\Phi$ is the derivative in the direction of slip

$$\partial^{(\beta)}\Phi = \boldsymbol{s}^{(\beta)} \cdot \boldsymbol{\nabla}\Phi. \tag{11}$$

Thus $\boldsymbol{G}$ may be viewed as representing an edge dislocation with Burgers vector $\boldsymbol{g}$ in the (x_1, x_2) plane and line direction $\boldsymbol{e}_3$. The Burgers vector resolved on slip system β has the form

$$\boldsymbol{g} \cdot \boldsymbol{s}^{(\beta)} = \sum_{\kappa} S^{(\beta\kappa)}\partial^{(\kappa)}\gamma^{(\kappa)}, \tag{12}$$

where $S^{(\beta\kappa)}$ is the slip-interaction coefficient

$$S^{(\beta\kappa)} = \boldsymbol{s}^{(\beta)} \cdot \boldsymbol{s}^{(\kappa)}. \tag{13}$$

3.2. Pile-up fields

We view $\partial^{(\beta)}\gamma^{(\beta)}$ (no sum over β!), as a macroscopic measure of the pile-up of dislocations on β.

For *double-slip* there is a one-to-one correspondence between the pile-up fields $\partial^{(\beta)}\gamma^{(\beta)}$ and the Burgers vector, since, by Eq. (10),

$$\boldsymbol{g} \cdot \boldsymbol{s}^{(1)} = \partial^{(1)}\gamma^{(1)} + S^{(12)}\partial^{(2)}\gamma^{(2)}, \quad \boldsymbol{g} \cdot \boldsymbol{s}^{(2)} = S^{(12)}\partial^{(1)}\gamma^{(1)} + \partial^{(2)}\gamma^{(2)}. \tag{14}$$

Because of this correspondence, the pile-ups can be expressed in terms of the resolutions $\boldsymbol{g} \cdot \boldsymbol{s}^{(\beta)}$:

$$\begin{aligned}
[1 - (S^{(12)})^2]\partial^{(1)}\gamma^{(1)} &= \boldsymbol{g} \cdot \boldsymbol{s}^{(1)} - S^{(12)}\boldsymbol{g} \cdot \boldsymbol{s}^{(2)}, \\
[1 - (S^{(12)})^2]\partial^{(2)}\gamma^{(2)} &= \boldsymbol{g} \cdot \boldsymbol{s}^{(2)} - S^{(12)}\boldsymbol{g} \cdot \boldsymbol{s}^{(1)}.
\end{aligned} \tag{15}$$

When there are more than two slip systems there is no such correspondence: while the pile-ups determine the Burgers vector via Eq. (10), the Burgers vector cannot uniquely determine the pile-ups. In fact, it is possible that a set of pile-ups, not all zero, correspond to a null Burgers vector.

4. Defect energies

We now discuss various specific choices for the defect energy. Throughout this discussion the constant $\ell > 0$ represents a constitutive length scale, generally different for each energy function.

4.1. Burgers-vector energies

We consider the following specific defect energies, here listed together with their associated microstresses.

(i) Isotropic energy (cf. Gurtin, 2002):

$$\Psi_{\mathrm{I}} = \tfrac{1}{2}\ell^2\pi_0|\boldsymbol{g}|^2, \quad \boldsymbol{\xi}^{(\beta)} = \ell^2\pi_0 \sum_{\kappa} S^{(\beta\kappa)}\partial^{(\kappa)}\gamma^{(\kappa)}\boldsymbol{s}^{(\beta)}. \tag{16}$$

(ii) Energy dependent on the resolved Burgers vector:

$$\Psi_S = \frac{1}{2}\ell^2\pi_0 \sum_{\beta,\kappa} k^{(\beta\kappa)} S^{(\beta\kappa)} (\boldsymbol{g}\cdot\boldsymbol{s}^{(\beta)})(\boldsymbol{g}\cdot\boldsymbol{s}^{(\kappa)}),$$
$$\boldsymbol{\xi}^{(\beta)} = \ell^2\pi_0 \sum_{\phi,\kappa,\rho} S^{(\beta\phi)} k^{(\phi\kappa)} S^{(\phi\kappa)} S^{(\kappa\rho)} \partial^{(\rho)}\gamma^{(\rho)}\boldsymbol{s}^{(\beta)}, \tag{17}$$

where

$$k^{(\beta\beta)} = 1 \quad \text{all } \beta, \quad k^{(\beta\kappa)} = k, \quad \beta \neq \kappa, \tag{18}$$

where k is a constant constitutive modulus. The presence of the factor $S^{(\beta\kappa)}$ ensures that Ψ_S be invariant to all symmetry transformations of the two-dimensional crystal. We also consider the special case in which $k = 0$, so that

$$\Psi_{S0} = \frac{1}{2}\ell^2\pi_0 \sum_{\beta} (\boldsymbol{g}\cdot\boldsymbol{s}^{(\beta)})^2, \quad \boldsymbol{\xi}^{(\beta)} = \ell^2\pi_0 \sum_{\rho,\phi} S^{(\beta\phi)} S^{(\phi\rho)} \partial^{(\rho)}\gamma^{(\rho)}\boldsymbol{s}^{(\beta)}. \tag{19}$$

The energy Ψ_S according to Eq. (17) will be referred to as the S energy, and Ψ_{S0} according to Eq. (19) as S0 energy.

4.2. Pile-up energy

The pile-up energy and associated microstress have the form

$$\Psi_P = \frac{1}{2}\ell^2\pi_0 \sum_{\beta} (\partial^{(\beta)}\gamma^{(\beta)})^2, \quad \boldsymbol{\xi}^{(\beta)} = \ell^2\pi_0 \partial^{(\beta)}\gamma^{(\beta)}\boldsymbol{s}^{(\beta)}. \tag{20}$$

Unlike energies dependent on the Burgers vector, the microstress for the pile-up energy does not couple the individual slip systems.

For *double-slip*, we may use Eq. (15) to conclude that

$$\frac{[1-(S^{(12)})^2]^2}{1+(S^{(12)})^2}\,[(\partial^{(1)}\gamma^{(1)})^2 + (\partial^{(2)}\gamma^{(2)})^2]$$
$$= (\boldsymbol{g}\cdot\boldsymbol{s}^{(1)})^2 + (\boldsymbol{g}\cdot\boldsymbol{s}^{(2)})^2 - \frac{4S^{(12)}}{1+(S^{(12)})^2}\,(\boldsymbol{g}\cdot\boldsymbol{s}^{(1)})(\boldsymbol{g}\cdot\boldsymbol{s}^{(2)}), \tag{21}$$

and hence that the pile-up energy is a special case of Eq. (17), albeit with a different ℓ.

5. Summary of DD results for single crystal thin films on a substrate

The problem of a thin film on a semi-infinite substrate subjected to thermal loading as illustrated in Fig. 1 has been studied using discrete-dislocation (DD) simulations by Nicola et al. (2003, 2005).

A quasi-static monotonic thermal loading is imposed by cooling the film–substrate system from an initial temperature T_0, at which film and substrate are stress free and dislocation free. The substrate undergoes unconstrained contraction but, due to the

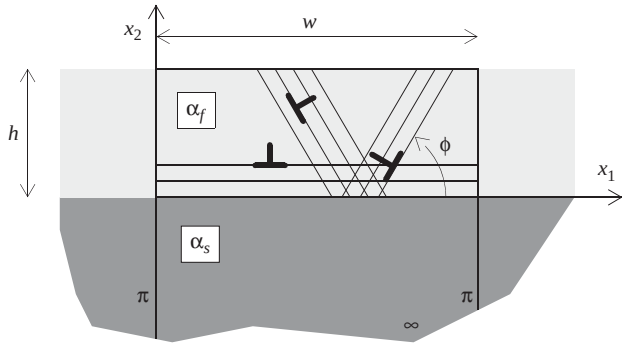

Fig. 1. Geometry of the film–substrate problem studied in this paper. A unit cell of width w is analyzed and the height of the substrate is taken large enough to represent a half-space.

mismatch between the thermal-expansion coefficient of film (α_f) and substrate (α_s), stress develops in the film; tensile for $\alpha_f > \alpha_s$. After an initial elastic response, dislocations nucleate in the film and partially relax the stress in the film by gliding on three sets of parallel slip planes. We focus on two crystal orientations: $\phi_{60} = (0^\circ, 60^\circ, 120^\circ)$ and $\phi_{30} = (30^\circ, 90^\circ, 150^\circ)$.

Results obtained for three different film thicknesses—$h = 1$, 0.5 and 0.25 μm—show that the average in-plane stress in the films is dependent on the film thickness. Results also show that hardening depends on crystal orientation: relaxation in films with orientation ϕ_{30} is higher than that in films with slip planes oriented ϕ_{60}. Moreover, the size effect is more evident for the ϕ_{60} orientation.

In both crystal orientations, the size dependence originates from the large stress gradient at the film–substrate interface, caused by dislocation pile-ups. Instead of a uniform stress distribution across the film height, as in the elastic state or according to classical local plasticity, the stress increases as the interface is approached, see Fig. 2a for ϕ_{30} and Fig. 3a for ϕ_{60}. The vertical lines in these figures indicate the average stress in each film, $\langle \sigma_{11} \rangle_f$. This data is tentatively fitted in Figs. 2b and 3b to power laws of the form $\sigma_{11} \propto h^{-p}$. Since different values of p are needed to fit the data, this type of power law seems inappropriate.

6. Closed-form solution of the thin film problem

We simplify the three-slip system model used in the DD simulations (Fig. 1) to one with only two slip systems. In the ϕ_{60} orientation, the slip plane parallel to the interface is hardly active and is therefore ignored. For the same reason, the 90° slip plane in the ϕ_{30} orientation is not considered in the application of the continuum theory. Thus, we consider the crystal to be oriented for symmetric double slip (see Fig. 4) with the angle $\phi^{(\beta)}$ between slip plane and film–substrate interface

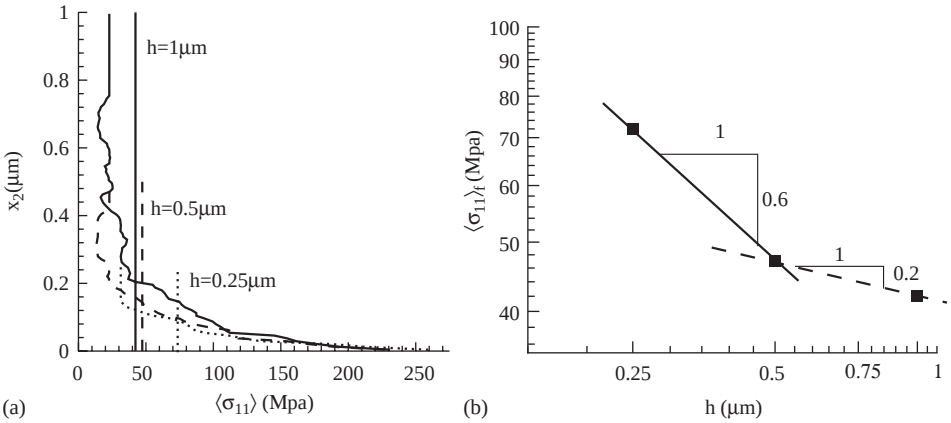

Fig. 2. DD results after cooling by 200 K for the crystal orientation with ϕ_{30} (Nicola et al., 2003). (a) Profiles across the film thickness of the in-plane stress in the films averaged along x_1. (b) Average film stress versus film thickness: data points are fitted two-by-two to a power law of the form $\langle\sigma_{11}\rangle_f \propto h^{-p}$.

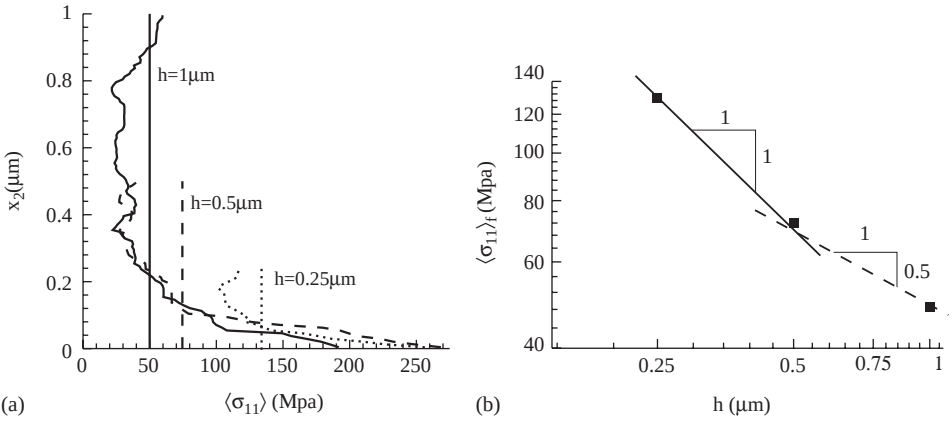

Fig. 3. DD results for ϕ_{60} (Nicola et al., 2003). (a) Profiles across the film thickness of the in-plane stress in the films averaged along x_1. (b) Average film stress versus film thickness with data points being fitted to a power law of the form $\langle\sigma_{11}\rangle_f \propto h^{-p}$.

being $\phi^{(1)} \equiv \phi$ and $\phi^{(2)} = \pi - \phi$. Then

$$\boldsymbol{s}^{(1)} = \cos\phi\boldsymbol{e}_1 + \sin\phi\boldsymbol{e}_2, \quad \boldsymbol{m}^{(1)} = -\sin\phi\boldsymbol{e}_1 + \cos\phi\boldsymbol{e}_2, \tag{22}$$

$$\boldsymbol{s}^{(2)} = -\cos\phi\boldsymbol{e}_1 + \sin\phi\boldsymbol{e}_2, \quad \boldsymbol{m}^{(2)} = -\sin\phi\boldsymbol{e}_1 - \cos\phi\boldsymbol{e}_2. \tag{23}$$

We consider traction-free, macroscopic conditions at the top of the film,

$$\sigma_{12}(x_1, h) = \sigma_{22}(x_1, h) = 0. \tag{24}$$

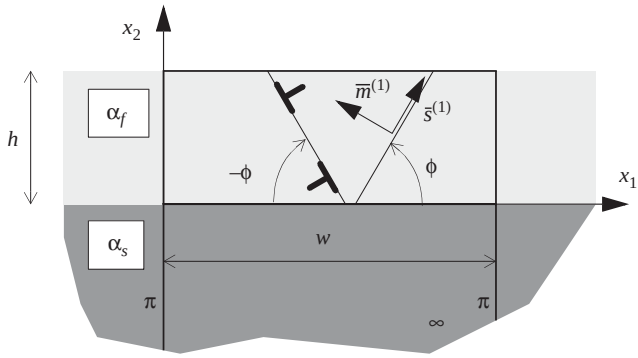

Fig. 4. Geometry of the thin film problem in symmetric double slip.

The additional, microscopic boundary conditions are the micro-free condition at the film top, where dislocations can freely leave the film, and the micro-clamped condition at the film–substrate interface, where slip cannot occur, i.e.

$$n_i \xi_i^{(\beta)}(x_1, h) = 0, \quad \gamma^{(\beta)}(x_1, 0) = 0. \tag{25}$$

Since the film is infinitely long in the x_1-direction and initially homogeneous, the solution depends only on x_2. With all stress components independent of x_1, equilibrium together with the macroscopic boundary conditions Eq. (24) requires that $\sigma_{12} = \sigma_{22} = 0$ throughout the film. The elastic solution is a spatially uniform field $\sigma_{11}(x_2) = \text{const.}$, so that yield takes place uniformly in the crystal when $\tau^{(\beta)} = |\pi_0|$ on both slip systems, with

$$\tau^{(1)} = -\tau^{(2)} = -\tfrac{1}{2}\sigma_{11} \sin 2\phi \equiv -\tau. \tag{26}$$

Because of the double-slip orientation and symmetry,

$$\gamma^{(1)} = -\gamma^{(2)} \equiv -\gamma, \tag{27}$$

where it is expected that $\gamma \geqslant 0$ since $\tau \geqslant 0$ if the film is in tension.

Because of Eq. (27), the yield conditions on the two slip systems lead to a single differential equation for $\gamma(x_2)$. The time derivative of this equation has the form

(i) for the isotropic energy (Eq. (16)),

$$\frac{\mathrm{d}^2 \dot{\gamma}}{\mathrm{d}x_2^2} = -\frac{\dot{\sigma}_{11}}{\ell^2 \pi_0 \sin 2\phi}, \tag{28}$$

(ii) for the S energy (Eq. (17)),

$$\frac{\mathrm{d}^2 \dot{\gamma}}{\mathrm{d}x_2^2} = -\frac{\dot{\sigma}_{11}}{(1 + k \cos 2\phi)\ell^2 \pi_0 \, 2 \sin 2\phi \cos^2 \phi}, \tag{29}$$

(iii) for the pile-up energy (Eq. (20)),

$$\frac{\mathrm{d}^2\dot{\gamma}}{\mathrm{d}x_2^2} = -\frac{\dot{\sigma}_{11}\cot\phi}{\ell^2\pi_0}, \tag{30}$$

where ℓ may vary between the three energy types. The stress field $\sigma_{11}(x_2)$ is nonuniform and unknown at this stage. Because of symmetry and because strain-rate components do not depend on x_1, $\dot{\varepsilon}_{11}$ must be uniform throughout the film. The total strain splits up into an elastic part, a plastic part and a thermal part given by $\varepsilon_{ij}^{\mathrm{T}} = (1+\nu)\alpha\Delta T\delta_{ij}$ (where the factor $(1+\nu)$ is a consequence of the plane strain formulation). Considering that the substrate expands by $\varepsilon_{11} = (1+\nu)\alpha_{\mathrm{s}}\dot{T}$, compatibility of deformation between the film and the substrate requires that $\dot{\varepsilon}_{11}$ is the same and uniform throughout the film. Hence,

$$(1+\nu)\alpha_{\mathrm{s}}\dot{T} = \dot{\varepsilon}_{11}^{\mathrm{e}} + \dot{\varepsilon}_{11}^{\mathrm{p}} + (1+\nu)\alpha_{\mathrm{f}}\dot{T}, \tag{31}$$

so that

$$(1+\nu)(\alpha_{\mathrm{s}} - \alpha_{\mathrm{f}})\dot{T} = \frac{(1-\nu^2)}{E}\,\dot{\sigma}_{11} + \dot{\gamma}\sin 2\phi. \tag{32}$$

Eliminating $\dot{\sigma}_{11}$ by means of Eq. (28), we obtain the following ordinary second-order differential equation for $\dot{\gamma}$:

$$\frac{\mathrm{d}^2\dot{\gamma}}{\mathrm{d}x_2^2} - \lambda^2\dot{\gamma} = -F, \tag{33}$$

with constant coefficients λ and F given through

$$\lambda^2 = \frac{E}{(1-\nu^2)\ell^2\pi_0 f(\phi)}, \quad F = \frac{E(\alpha_{\mathrm{s}} - \alpha_{\mathrm{f}})\dot{T}}{(1-\nu)\ell^2\pi_0 \sin 2\phi f(\phi)}. \tag{34}$$

Here, $f(\phi)$ is a function of orientation ϕ which, depending on the energy considered, takes the following forms:

(i) for the isotropic energy (Eq. (16)),

$$f(\phi) = 1, \tag{35}$$

(ii) for the S energy (Eq. (17)),

$$f(\phi) = (1 + k\cos 2\phi)2\cos^2\phi, \tag{36}$$

(iii) for the pile-up energy (Eq. (20)),

$$f(\phi) = \frac{1}{2\cos^2\phi}. \tag{37}$$

Dependence on the dissipative hardening modulus H_0 was found to be so weak that the solution is here given for[1]

$$H_0 = 0.$$

Solving Eq. (33) subject to the microscopic boundary conditions (25) and (26) we obtain the solution

$$\dot{\gamma} = \frac{F}{\lambda^2}\,[1 - \cosh \lambda x_2 + \tanh \lambda h \sinh \lambda x_2], \tag{38}$$

where, for all energies,

$$\frac{F}{\lambda^2} = \frac{(1+\nu)(\alpha_s - \alpha_f)\dot{T}}{\sin 2\phi}. \tag{39}$$

Substituting Eq. (38) back into Eq. (32), we find a linear relation between $\dot{\sigma}_{11}$ and $\dot{T}$, which, after integration from the onset of yield (at temperature $T_y < T_0$) to the current temperature T, gives

$$\sigma_{11} = \sigma_y + (\sigma_n - \sigma_y)[\cosh \lambda x_2 - \tanh \lambda h \sinh \lambda x_2]. \tag{40}$$

Here,

$$\sigma_y = -\frac{E}{1-\nu}\,(\alpha_f - \alpha_s)(T_y - T_0), \quad \sigma_n = -\frac{E}{1-\nu}\,(\alpha_f - \alpha_s)(T - T_0), \tag{41}$$

respectively, are the (uniform) film stress at the onset of yield (at temperature T_y) and the stress in the absence of plasticity. The solutions for the different defect energies differ only through the ϕ dependence of λ.

7. Comparison of the gradient theory with DD simulations

The closed-form expression for the stress distribution (40) can be readily integrated over the film thickness to give the film-average stress as a function of h. The solution depends on the values of a number of material parameters. For the elastic constants, we take the characteristic values for aluminum ($E = 70\,\text{GPa}$ and $\nu = 0.33$) adopted in the DD simulations presented in Section 5, and the same coefficients of thermal expansion. The initial shear strength π_0 is taken from the DD results to be $\pi_0 = 15.5\,\text{MPa}$, corresponding to a film stress of $4/\sqrt{3}\pi_0 = 36\,\text{MPa}$ (Nicola et al., 2003). Yield in the DD simulations is determined by the strength of the weakest dislocation source. The values of the source strengths in the simulations were chosen out of a Gaussian distribution with average $\tau_{nuc} = 25\,\text{MPa}$ and a standard deviation of 5 MPa.

[1]The modulus H_0 has no direct counterpart in the DD simulations, because the film barely hardens in tension when not on a substrate (see Nicola et al., 2005). Moreover, the exact solution when generalized to $H_0 \neq 0$ turns out to be essentially independent of H_0 for $H_0 < 100\,\text{MPa}$.

7.1. The isotropic energy

For the isotropic energy, the only free parameter is the length scale ℓ originating from Eq. (16). It is clear from Eq. (40) that the DD results for the two crystal orientations cannot be fitted using a single value of the material parameter ℓ: the equation depends on ϕ only through $\sin 2\phi$, which is the same number for $\phi = 60^\circ$ and 30°. A value of $\ell = 1.8\,\mu\text{m}$ gives a $\langle\sigma_{11}\rangle_f$–$h$ curve which agrees quite well with the DD data points in the case of ϕ_{30}, as shown in Fig. 5b. We tried, without success, to find a value of ℓ giving a similar fit to the $\langle\sigma_{11}\rangle_f$–$h$ dislocation data for the slip plane orientation with ϕ_{60}. Fig. 6b shows three curves for $\ell = 2$, 3 and $4\,\mu\text{m}$, each of them agreeing only with the DD data for a single particular thickness h. Figs. 5a and 6a show the stress profiles across the film height according to Eq. (40), which indeed exhibit a stress gradient. Another noteworthy feature of the solution is that the stress at the film–substrate interface is independent of h, and equal to the elastic stress σ_n, Eq. (41). Fig. 7, finally shows the stress–temperature curves given by solution (40), which reinforces the difficulties in obtaining a good fit for ϕ_{60}.

7.2. The S0 defect energy

The solution for this energy also has only the length scale ℓ as a free material parameter. For $\ell = 1.5\,\mu\text{m}$, it is possible to fit the DD results for the ϕ_{30} orientation, but the solution for the same material length scale for the orientation ϕ_{60} does not match the DD results. The curves in Fig. 8 show an opposite trend with respect to the DD predictions: the size effect is smaller for the ϕ_{60} orientation than for the ϕ_{30}.

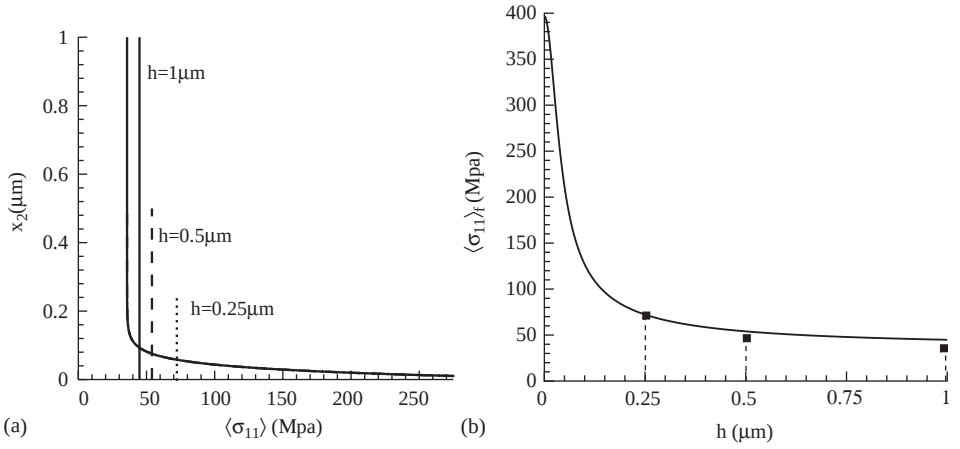

Fig. 5. Predictions using the isotropic defect energy, Eq. (16), for $\phi = 30^\circ$ with $\ell = 1.8\,\mu\text{m}$ at the same final temperature as in Fig. 2. (a) Profiles of the in-plane stress across the film thickness. Vertical lines indicate the average stress in the films, which are plotted in (b) as a function of film thickness h (scaling behavior $\langle\sigma_{11}\rangle_f \propto \tanh \lambda h/\lambda h$). Square symbols indicate the data points from the DD simulations.

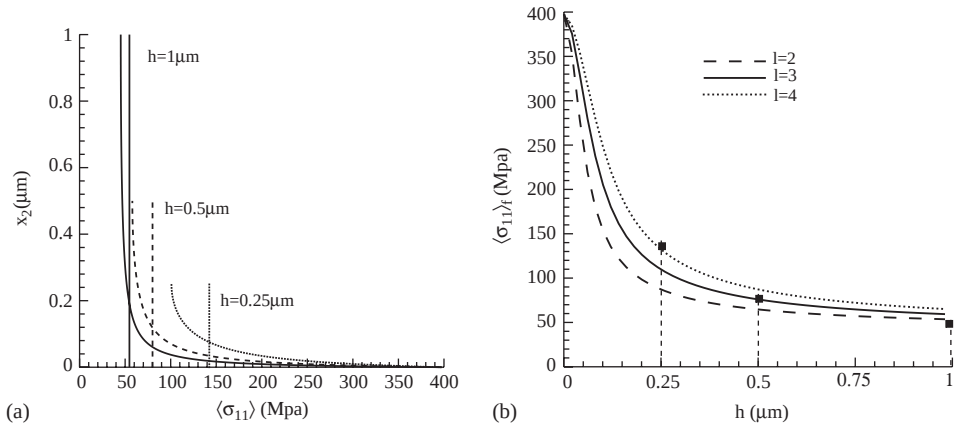

Fig. 6. Predictions using the isotropic defect energy, Eq. (16), for $\phi = 60^\circ$ at the same final temperature as in Fig. 3. (a) Profiles of the in-plane stress across the film thickness with $\ell = 1.8\,\mu$m. (b) The average film stress as a function of film thickness h for three values of ℓ: $\ell = 2$, 3 and 4 μm. Square symbols indicate the data points from the DD simulations.

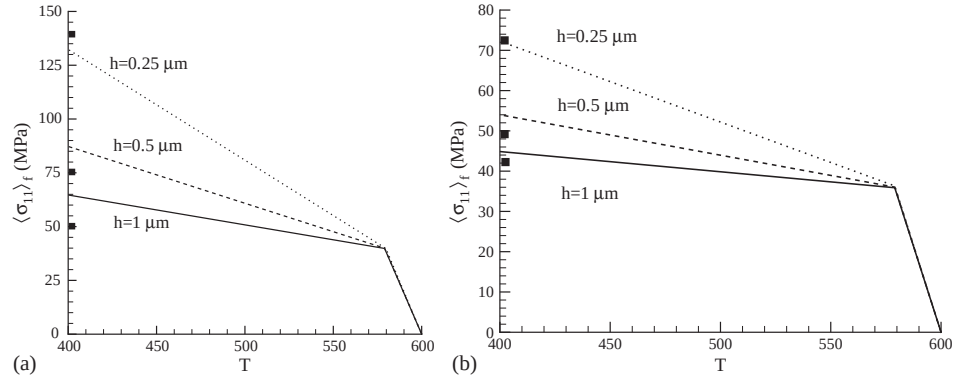

Fig. 7. Film-average stress–temperature curves according to the strain gradient solution Eq. (40) using the isotropic defect energy, Eq. (16), for (a) $\phi = 30^\circ$ with $\ell = 1.8\,\mu$m and (b) for $\phi = 60^\circ$ with $\ell = 4\,\mu$m. Square symbols indicate the stress at final temperature in the DD simulations, as shown also in Figs. 2, 5 and 3, 6.

7.3. The S defect energy

In this case, with $f(\phi)$ according to Eq. (36), there is an additional free parameter, k, beside the material length scale ℓ. While positive values of k give similar trends as the ones obtained with the S0 defect energy, i.e. a smaller size effect for the ϕ_{60} orientation than for the ϕ_{30}, a negative k gives the opposite trend,

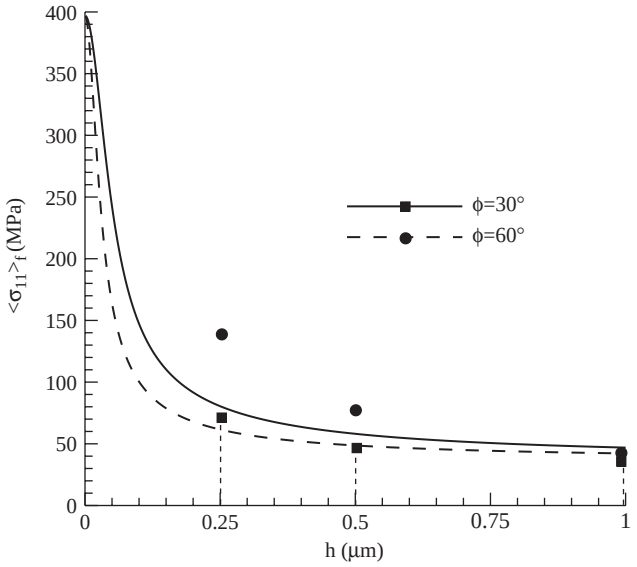

Fig. 8. Average stress in the films versus film thickness h predicted for the S0 defect energy, Eq. (19), for $\phi = 30^\circ$ and 60°. The symbols represent the DD results.

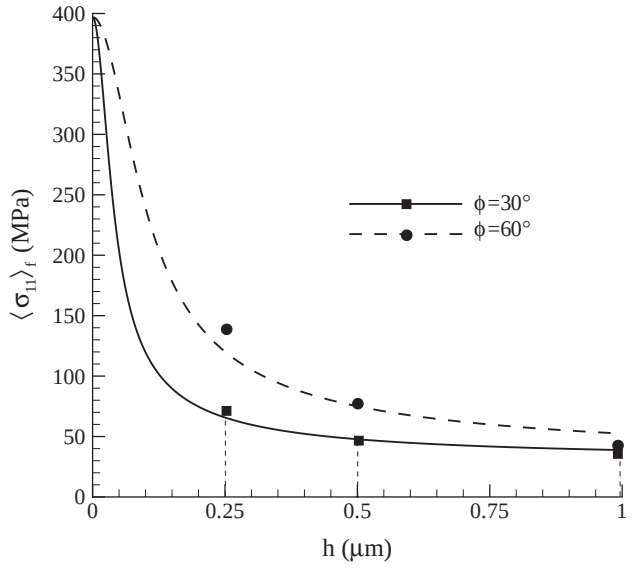

Fig. 9. Film-average tensile stress as a function of film thickness h for two orientations according to the S theory for $k = -1.8$ and $\ell = 4.5\,\mu\text{m}$.

i.e. in agreement with the DD results. There is no unique set of values for k and ℓ, but the results obtained for $k = -1.8$ and $\ell = 4.5\,\mu\text{m}$ shown in Fig. 9 provides the best fit.

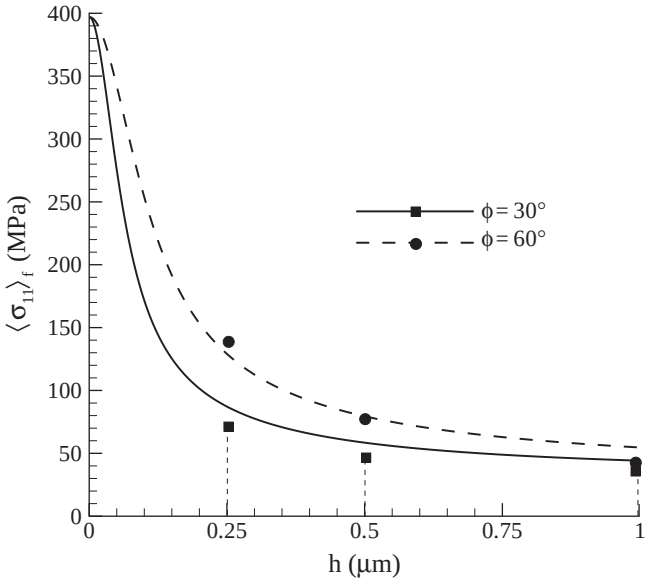

Fig. 10. Film-average tensile stress as a function of film thickness h for two orientations according to the pile-up theory for $\ell = 3\,\mu\text{m}$.

7.4. The pile-up defect energy

By considering the free energy in the form of the pile-up defect energy, Eq. (20), we again have only one free material parameter for the fit with the simulations, ℓ. Even though the fit seen in Fig. 10 is not quite as good as the one obtained for the S energy, there still is a quite good agreement for $\ell = 3\,\mu\text{m}$. It is worth noting that the S energy reduces to the S0-energy for $k = 0$, and to the pile-up energy for $k = -2/(1+\cos^2 2\phi)$ $(k_{30} = k_{60} = -\frac{8}{5})$ and for $\ell_S = \ell_P\sqrt{1+\cos^2 2\phi}/(1-\cos^2 2\phi) \simeq 1.5\ell_P$. These relations follow directly from Eq. (21) since $S^{(12)} = -\cos 2\phi$ for this problem. The value $\ell_P = 3\,\mu\text{m}$ corresponds to $\ell_S = 4.5\,\mu\text{m}$ and $k = -1.6$. If these values were used in Fig. 9, we would find the same fit as in Fig. 10.

8. Conclusions

The problem of a thin film strained by a large substrate during cooling has been studied by discrete-dislocation simulations and by strain-gradient theory using a variety of constitutive equations for the defect energy. The latter vary in the way in which the slip gradient is assumed to affect the defect energy: either through the Burgers vector or through the pile-up field. Attention has been focused on the capability of the theory to capture the orientation-dependent size effect in thin films as captured by the simulations. The outcome of the study shows that the isotropic

energy, proposed previously in Gurtin (2002) and the S0 energy are not viable as general energies. For the limited comparison presented here, the P and S energies give good results, with the S energy slightly better than the P energy, at the expense of an extra material parameter.

The difference between the two energy functions is that the S energy depends on slip-resolved components of the Burgers vector while the P energy depends on pile-up fields. In the special case of double slip, the two energies can be made to coincide by proper choice of the constitutive moduli, but in general, these energy functions are different. It remains to be seen, for instance, by additional comparisons with other problems, which of the two energies is the most appropriate for plasticity at (sub-)micrometer scales.

It is worth noting that according to the discrete-dislocation simulations (Nicola et al., 2003, 2005) the origin of hardening in the thinnest film with ϕ_{60} is to a large extent nucleation controlled. In contrast, the strain-gradient theory, like all phenomenological continuum plasticity theories, is based on the assumption that dislocations are always available when required for stress relaxation. This is a possible reason for the fit between theory and discrete-dislocation not being as good in the ϕ_{60} orientation as in the ϕ_{30} orientation.

References

Aifantis, E.C., 1992. On the role of gradients in the localization of deformation and fracture. Int. J. Eng. Sci. 30, 1279–1299.

Bittencourt, E., Needleman, A., Gurtin, M.E., Van der Giessen, E., 2003. A comparison of nonlocal continuum and discrete dislocation plasticity predictions. J. Mech. Phys. Solids 51, 281–310.

Gudmundson, P., 2004. A unified treatment of strain gradient plasticity. J. Mech. Phys. Solids 52, 1379–1406.

Gurtin, M.E., 2002. A gradient theory of single-crystal viscoplasticity that accounts for geometrically necessary dislocations. J. Mech. Phys. Solids 50, 5–32.

Hutchinson, J.W., 2000. Plasticity at the micron scale. Int. J. Solid Struct. 37, 225–238.

Needleman, A., 2000. Computational mechanics at the mesoscale. Acta Mater. 48, 105–124.

Nicola, L., Van der Giessen, E., Needleman, A., 2003. Discrete dislocation analysis of size effects in thin films. J. Appl. Phys. 93, 5920–5928.

Nicola, L., Van der Giessen, E., Needleman, A., 2005. Two hardening mechanisms in single-crystal thin films studied by discrete-dislocation plasticity. Philos. Mag., in press.

Svendsen, B., 2002. Continuum thermodynamic models for crystal plasticity including the effects of geometrically necessary dislocations. J. Mech. Phys. Solids 50, 1297–1329.